Skeletal Radiol
DOI 10.1007/s00256-012-1516-0

SCIENTIFIC ARTICLE

CT arthrography of the wrist using a novel, mobile, dedicated extremity cone-beam CT (CBCT)

Seppo K. Koskinen · Ville V. Haapamäki · Jari Salo · Nina C. Lindfors · Mika Kortesniemi · Lauri Seppälä · Kimmo T. Mattila

Received: 11 June 2012 / Revised: 17 August 2012 / Accepted: 27 August 2012

Abstract
Purpose To evaluate the feasibility and intra- and interobserver agreement of CBCT arthrography of wrist ligaments, triangular fibrocartilaginous complex (TFCC), and to assess the sensitivity (SE), specificity (SP), accuracy (ACC), and positive and negative predictive value (PPV, NPV) of CBCT arthrography in the diagnosis of scapholunate (SLL) and lunotriquetral (LTL) ligament tears, TFCC, and cartilage abnormalities of the scaphoid and lunate with their corresponding radial surfaces (scaphoid and lunate fossa) using a novel, mobile, dedicated extremity CBCT scanner.
Materials and methods Fifty-two consecutively enrolled subjects (26 M, 26 F, mean age 38 years, range 18–66 years) with suspected wrist ligament tears underwent CBCT-arthrography before normally scheduled MR arthrography.An extremity CBCT was used for imaging with isotropic voxel size of $0.4 \times 0.4 \times 0.4\ mm^3$. Subsequent routine 1.5 T MRI was performed using a dedicated wrist coil.Two observers reviewed the anonymized CBCT images twice for contrast enhancement (CE) and technical details (TD), for tears of the SLL, LTL, and TFCC. Also, cartilage abnormalities of the scaphoid and lunate with their corresponding radial surfaces (scaphoid and lunate fossa) were evaluated. Inter- and intraobserver agreement was determined using weighted kappa statistics. Since no surgery was performed, MRI served as a reference standard, and SE and SP, ACC, PPV, and NPV were calculated.
Results Intra- and interobserver kappa values for both readers (reader 1/reader 2; first reading/second reading) with 95 % confidence limits were: CE 0.54 (0.08–1.00)/ 0.75 (0.46–1.00); 0.73 (0.29–1.00)/ 0.45 (0.07–0.83), TD 0.53 (0.30–0.88)/ 0.86 (0.60–1.00); 0.56 (0.22–0.91)/ 0.67 (0.37–0.98), SLL 0.59 (0.25–0.93)/ 0.66 (0.42–0.91); 0.31 (0.06–0.56)/ 0.49 (0.26–0.73), LTL 0.83 (0.66–1.00)/ 0.68 (0.46–0.91); 0.90 (0.79–1.00)/ 0.48 (0.22–0.74); TFCC (0.72–1.00)/ (0.79–1.00); 0.65 (0.43–0.87)/ 0.59 (0.35–0.83), radius (scaphoid fossa) 0.45 (0.12–0.77)/ 0.64 (0.31–0.96); 0.58 (0.19–0.96)/ 0.38 (0.09–0.66), scaphoid

S. K. Koskinen · V. V. Haapamäki · M. Kortesniemi
Department of Radiology, HUS Helsinki Medical Imaging Center, Helsinki University Central Hospital, Helsinki, Finland

J. Salo
Department of Orthopedic and Trauma Surgery, Helsinki University Central Hospital, Helsinki, Finland

J. Salo
Department of Orthopedics, Traumatology and Hand Surgery, Kuopio University Hospital, UEF, Kuopio, Finland

N. C. Lindfors
Department of Orthopedic and Hand Surgery, Helsinki University Central Hospital, Helsinki, Finland

L. Seppälä
Planmed Oy, Helsinki, Finland

K. T. Mattila
Department of Diagnostic Radiology, Turku University Central Hospital, Turku, Finland

S. K. Koskinen (✉)
Department of Radiology, HUS Helsinki Medical Imaging Center, Helsinki University Hospital, Töölö Trauma Center, Topeliuksenkatu 5, PL 266, Helsinki 00029 Finland
e-mail: seppo.koskinen@helsinki.fi

Published online: 19 September 2012

0.43 (0.12–0.74)/ 0.76 (0.55–0.96); 0.37 (0.00–0.75)/ 0.32 (0.04–0.59), radius (lunate fossa) 0.68 (0.36–1.00)/ 0.42 (0.00–0.86); 0.62 (0.29–0.96)/ 0.51 (0.12–0.91), and lunate 0.53 (0.16–0.90)/ 0.68 (0.44–0.91); 0.59 (0.29–0.88)/ 0.42 (0.00–0.84), respectively.

The overall mean accuracy was 82–92 % and specificity was 81–94 %. Sensitivity for LTL and TFCC tears was 76–83, but for SLL tears it was 58 %. For cartilage abnormalities, the accuracy and negative predictive value were high, 90–98 %.

Conclusions A dedicated CBCT extremity scanner is a new method for evaluating the wrist ligaments and radiocarpal cartilage. The method has an overall accuracy of 82–86 % and specificity 81–91 %. For cartilage abnormalities, the accuracy and negative predictive value were high.

Keywords Wrist · Arthrogram · Cone beam CT · Trauma · Musculoskeletal

Introduction

Magnetic resonance arthrography is an established technique for detecting ligament and cartilage injuries of the wrist [1–3]. However, the technique is rather expensive and time-consuming, and MRI in general has several contraindications. Also, spatial resolution of MRI can be a limiting factor, especially in areas of convex or concave joint facets with thin cartilage [4, 5]. Therefore, alternative techniques such as CT arthrography (CTA) have received more attention [6]. CTA is a much faster technique and has excellent spatial resolution [7]. Moreover, the ability for multiplanar reformats makes it even more versatile. In addition to conventional CT scanners, cone-beam CT (CBCT) has been used for dental imaging since the late 1990s [8, 9]. The clinical indications include dentoalveolar imaging, such as assessing dentoalveolar trauma and preoperative assessment of impacted teeth, and preoperative planning for maxillofacial surgery [10]. This method has recently been implemented in orthopedic imaging to study finger and wrist fractures and scaphoid fracture after screw fixation [11, 12]. More recently, dedicated extremity CBCT scanners have been introduced [13, 14]. This application offers an attractive alternative, with high spatial resolution, easy installation, and low radiation dose [4, 11–15] compared to conventional CT scanners. Also, the ability to image the lower extremity during weight bearing, i.e., while the patient stands, opens new possibilities to study degenerative joint disease of the knee, ankle, and foot (Tuominen et al., Weight bearing CT-imaging of the lower extremity, unpublished).

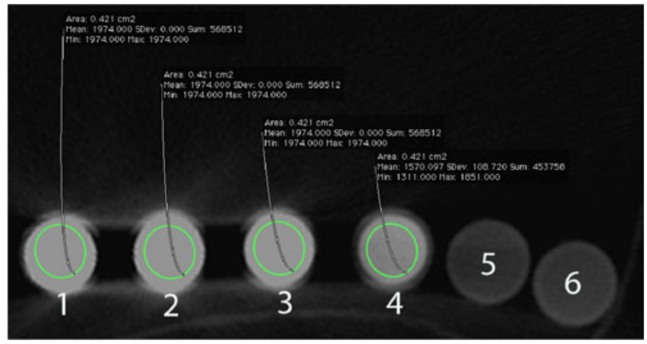

Fig. 1 CBCT image (88 kVp, 8 mA) of six phantoms of 2-ml volume with varying proportions of 240 mg I/ml iohexol and 2.5 mmol/l tetraazacyclododecanetetraacetic acid (DOTA)-gadolinium in the following respective proportions: 1 phantom 1,100 %/0 %; phantom 2, 75 %/25 %; phantom 3, 50 %/50 %; phantom 4, 25 %/75 %; phantom 5, 0 %/100 %, and phantom 6100 % isotonic NaCl. Using the mixture of 50/50 (3), there was no decrease in attenuation values as there was with the concentration of 25/75 (4)

In this study, we wanted to expand the dedicated extremity CBCT scanner's capabilities even further, i.e., with CT arthrography. Therefore, the purpose of this study was to evaluate the feasibility and intra- and interobserver agreement of CT arthrography of scapholunate and lunotriquetral ligaments, triangular fibrocartilaginous complex, and cartilage abnormalities using a novel, dedicated extremity CBCT. To our knowledge, this is the first report of wrist arthrography using a dedicated extremity CBCT scanner.

Materials and methods

Fifty-three consecutively enrolled subjects were offered a CBCT arthrogram immediately prior to their routinely

Fig. 2 The hand and wrist can be placed freely in any desired position

scheduled MRI arthrogram. The time period was 7 months, from November 2010 to May 2011. One patient refused to participate in the study and hence the final study group was comprised of 52 subjects (26 M, 26 F, mean age 38 years, range 18–66 years). Approval was obtained from the hospital's ethics committee, and written informed consent was obtained from each subject.

The indication for MR arthrography was suspected scapholunate (SL) ligament tear in 17 subjects, lunotriquetral (LT) ligament tear (n=1), SL and LT ligament tear (n=8), SL and triangular fibrocartilage complex (TFCC) tear (n=2), LT and TFCC tear (n=2), TFCC tear (n=19). In addition, radiocarpal joint cartilage assessment was requested in six cases, and evaluation of distal radioulnar joint (DRUJ) in two cases. Five patients were operated on within the last 12 months (Brunelli's tenodesis for scapholunate instability, STT-arthrodesis + TFCC fixation, fixation of distal radius fracture with volar plate (n=2), resection of pisiform bone), and one patient had undergone a diagnostic wrist arthroscopy 12 months earlier. Moreover, one patient had avascular necrosis with fragmentation of the lunate.

Since the patients underwent subsequent MRI arthrography of the wrist, we first studied the amount of CT and MR contrast used in the mixture to obtain optimal contrast. We prepared six phantoms of 2-ml volume with varying proportions of 240 mg I/ml iohexol (Omnipaque, GE Healthcare, Oslo, Norway) and 2.5 mmol/l tetraazacyclododecanetetraacetic acid (DOTA)-gadolinium (Artirem, Guerbet, France). Phantoms 1–5 were composed of 240 mg I/ml iohexol and 2.5 mmol/l DOTA-gadolinium in the following respective proportions: phantom 1,100 %/0 %; phantom 2, 75 %/25 %; phantom 3, 50 %/50 %; phantom 4, 25 %/75 %; phantom 5, 0 %/100 %, and phantom 6 100 % isotonic NaCl. The mixture of 1:1 was selected, because it provided adequate contrast for both in vitro and in vivo CBCT (Fig. 1) and MR arthrography images.

A mean of 2.2 ml (range 1.5–3.0 ml) of 1:1 solution of 2.5 mmol/l Gd- DOTA and 240 mg I/ml iohexol was injected into the radiocarpal joint under palpation guidance.

A novel extremity CBCT scanner (Planmed Verity, Planmed Oy, Helsinki, Finland) was used to image the wrist (Fig. 2). The dimensions of the scanner are (L × W × H): 185 × 76 × 160 cm, weight app. 350 kg, maximum power-consumption 1.5 kVA with no external cooling needed. The scanner uses a Toshiba X-ray tube with a tungsten target, anode voltage up to 96 kV, anode current 1–12 mA, dual filtration 0.5 mm-Cu + 2.5 mm-Al, and pulsed X-ray radiation. The scanner has a 20 × 25-cm flat-panel amorphous silicon detector. The field of view (FOV) is approximately 13 × 16 cm, and 300 projection images were acquired over an angle of 210° with a scan time of 18 s and reconstruction time of 30–120 s. The isotropic voxel size was 0.4 × 0.4 × 0.4 mm^3. Based on previous tests [14], 88 kVp

Table 1 Intra- and interobserver kappa values for readers 1 (R1) and 2 (R2) for contrast enhancement (CE), technical details (TD), for tears of scapholunate (SLL) and lunotriquetral (LTL) ligament, and triangular fibrocartilaginous complex (TFCC) and for cartilage for scaphoid and lunate with corresponding radial surface. R1.1 and R2.1 denote the first and second reader's first reading, and R1.2 and R2.2 the second readings, respectively. The 95 % confidence intervals are shown in *parentheses*

	Intraobserver	Interobserver
CE	R1 0.54 (0.08–1.00)	R1.1-R2.1 0.73 (0.29–1.00)
	R2 0.75 (0.46–1.00)	R1.2-R2.2 0.45 (0.07–0.83)
TD	R1 0.53 (0.30–0.88)	R1.1-R2.1 0.56 (0.22–0.91)
	R2 0.86 (0.60–1.00)	R1.2-R2.2 0.67 (0.37–0.98)
SLL	R1 0.59 (0.25–0.93)	R1.1-R2.1 0.31 (0.06–0.56)
	R2 0.66 (0.42–0.91)	R1.2-R2.2 0.49 (0.26–0.73)
LTL	R1 0.83 (0.66–1.00)	R1.1-R2.1 0.90 (0.79–1.00)
	R2 0.68 (0.46–0.91)	R1.2-R2.2 0.48 (0.22–0.74)
TFCC	R1 0.86 (0.72–1.00)	R1.1-R2.1 0.65 (0.43–0.87)
	R2 0.91 (0.79–1.00)	R1.2-R2.2 0.59 (0.35–0.83)
RADIUS (scaphoid fossa)	R1 0.45 (0.12–0.77)	R1.1-R2.1 0.58 (0.19–0.96)
	R2 0.64 (0.31–0.96)	R1.2-R2.2 0.38 (0.09–0.66)
SCAPHOID	R1 0.43 (0.12–0.74)	R1.1-R2.1 0.37 (0.00–0.75)
	R2 0.76 (0.55–0.96)	R1.2-R2.2 0.32 (0.04–0.59)
RADIUS (lunate fossa)	R1 0.68 (0.36–1.00)	R1.1-R2.1 0.62 (0.29–0.96)
	R2 0.42 (0.00–0.86)	R1.2-R2.2 0.51 (0.12–0.91)
LUNATE	R1 0.53 (0.16–0.90)	R1.1-R2.1 0.59 (0.29–0.88)
	R2 0.68 (0.44–0.91)	R1.2-R2.2 0.42 (0.00–0.84)

and 8 mA were used, giving a DAP of 716 mGycm^2. The small size enabled the scanner to be installed in the general X-ray room.

After CBCT, the patients were transferred to the MRI suite within 15 min post-injection. For MRI, we used a 1.5-T scanner (Signa HD, GE Medical Systems, Milwaukee, WI, USA) using the following imaging parameters: coronal T1 SE (TR/TE 620/13 ms, slice thickness 2.5 mm/2.7 space, matrix 256 × 192), axial T2 FSE fat-saturated MR images (TR/TE eff. 2800/44 ms, slice thickness 3 mm/3.3 mm space, ETL 8, matrix 320 × 192), and coronal T2-w fat-saturated FSE (TR/TE eff. 2760/68 ms, ETL 10, slice thickness 2.5 mm/2.7 space, matrix 288 × 192). FOV was 10 cm in each sequence.

The images were transferred to a 27″ iMac computer (Mac OS 10.6.4, Cupertino, CA, USA) and analyzed using Aycan OsirixPro (v. 1.3, English Edition, January 2010, Aycan Digital Systems GmbH, Würzburg, Germany) software. Before the final analysis, the studies were anonymized and assigned a random ID number generated using freeware obtained at http://www.random.org/.

A month later, two radiologists with more than 5 years of experience in musculoskeletal (MSK) trauma imaging using CT and MRI reviewed the CBCT images twice with a minimum 2-week interval between evaluations, for contrast enhancement (CE; 1=good, 2=fair; 3=poor) and technical details (TD; 1=good, 2=motion, 3=suboptimal contrast injection). Also, evidence of tears of scapholunate (SLL) and lunotriquetral (LTL) ligaments (1=no tear, 2=completely torn, 3=partial tear) and triangular fibrocartilaginous complex (TFCC) (1=no tear, 2=torn) and cartilage abnormalities (1=normal, 2=thinning, 3=exposed subchondral bone) for scaphoid and lunate with corresponding radial surface (scaphoid and lunate fossa) were evaluated.

For MRI analysis, we used standard clinical workstations (Agfa DS3000, IMPAX 5.3, Agfa-Gaevert, Mortsel, Belgium) with 2-megapixel monitors (Barco Inc., Kortrijk, Belgium).

Inter- and intraobserver agreement was determined using weighted kappa statistics. In this study, it was defined that kappa-values 0.01–0.20 mean slight agreement, 0.21–0.40 fair agreement, 0.41–0.60 moderate agreement, 0.61–0.80 substantial agreement, and 0.80–0.99 almost perfect agreement [16]. Since no surgery was performed, the consensus MRI reading served as a reference standard, and sensitivity (SE), specificity (SP), accuracy (ACC), and positive and negative predictive values (PPV, NPV) were calculated.

Statistical analyses were done using a commercial software package SAS/STAT v.9.2 (SAS Institute Inc., Cary, NC, USA).

Results

Each CBCT imaging study was technically successful. In two patients, the contrast was suboptimal; in one case most likely due to previous fracture fixation, in the other case due to technical difficulties during injection. Also, in two patients with radial volar titanium plate and screws, the metal artifact caused less diagnostic problems in the assessment of both the wrist cartilage and ligament structures in CBCT images compared to the MRI.

Interobserver agreement for SL ligament was fair. Moderate agreement was seen on articular cartilage for radius, scaphoid, and lunate, and substantial agreement for LT

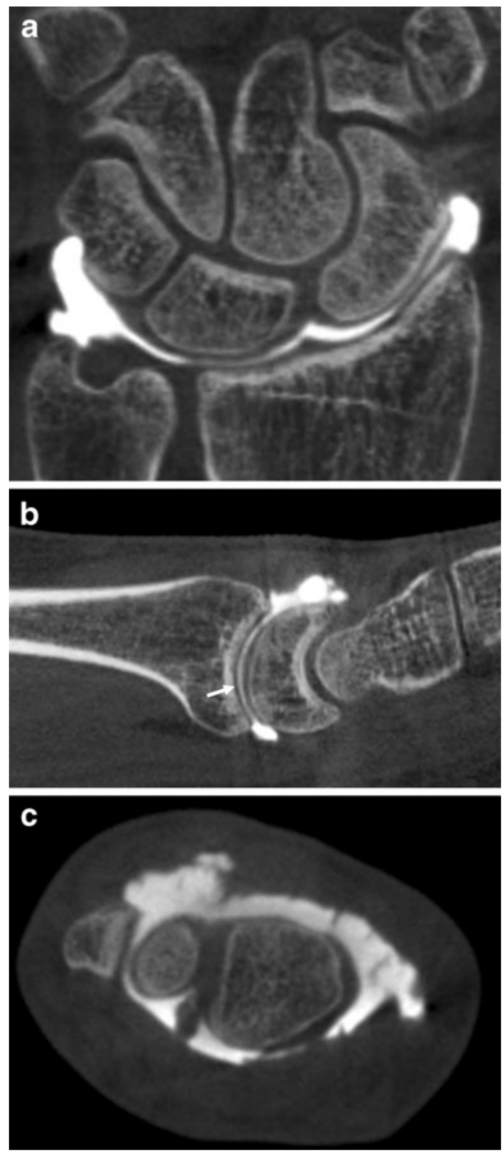

Fig. 3 Coronal (**a**), sagittal (**b**), and axial (**c**) images of the wrist. Voxel size 0.4 × 0.4 × 0.4 mm^3. Note the excellent visualization of cartilage surface in radial and lunate cartilage (*arrow*, **b**)

ligament and TFCC. Intraobserver agreement for TFCC was almost perfect (Table 1).

Image quality is demonstrated in Fig. 3

We found 11 SLL tears (ten total, one partial), seven LTL tears (five total, two partial), and 25 TFCC degenerations or tears according to Palmer classification (type 1A; 16, 1B; 2, 2A; 2, 2B 3; 2C; 2 and 2D 2) (Figs. 4, 5, and 6). For cartilage abnormalities, there were four cartilage abnormalities (thinning or subchondral bone exposure) for radial surface facing scaphoid (scaphoid fossa) and in scaphoid, six in lunate, and five in corresponding radial surface (lunate fossa).

The mean values for SE, SP, ACC, PPV, and NPV for SLL tears were 56, 91, 83, 67, and 89 %; for LTL tears 83, 81, 82, 44, and 96 %; for TFCC tears 76, 90, 87, 83, and 87 %, respectively. The results for each reader are presented in Table 2.

The mean values for SE, SP, ACC, PPV, and NPV for cartilage abnormalities for radial surface facing were 69, 94, 92, 53, and 97 %; for scaphoid 71, 94, 92, 61, and 97 %; for lunate fossa 63, 92, 90, 28, and 98 %; and for lunate 70, 92, 90, 52, and 97 %, respectively. The results for each reader are presented in Table 3.

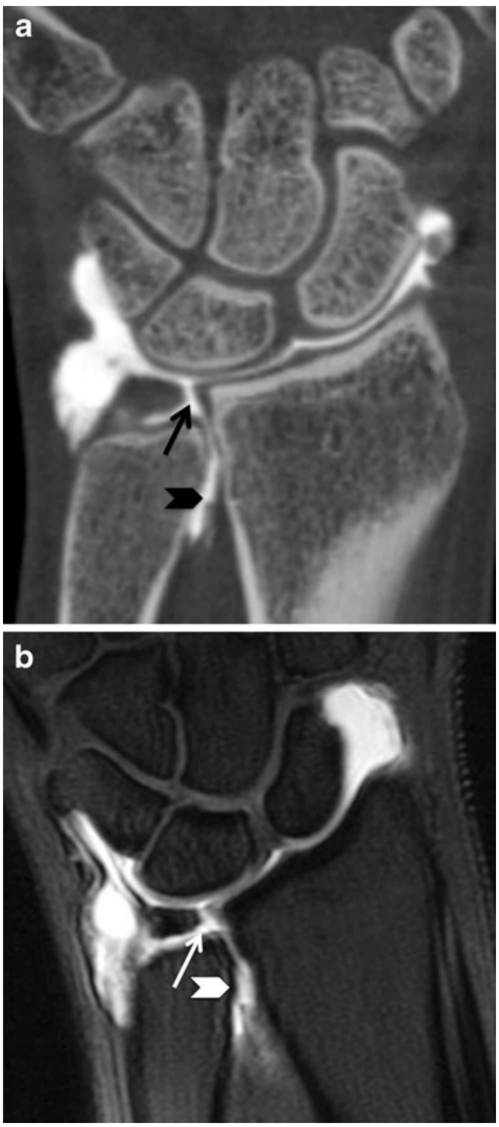

Fig. 4 TFC 1A tear (*arrow*). **a** Coronal CT-image (pixel size 0.4 × 0.4 × 0.4 mm^3) with **b** corresponding T2-w fat-saturated FSE MR image (TR/TE eff. 2,760/68 ms, ETL 10, FOV 10 cm, 3 mm/3.2 space, matrix 288 × 192). *Arrowhead* in **a** and **b** denotes contrast in distal radioulnar joint indicating communication between radiocarpal and distal radioulnar joint compartments

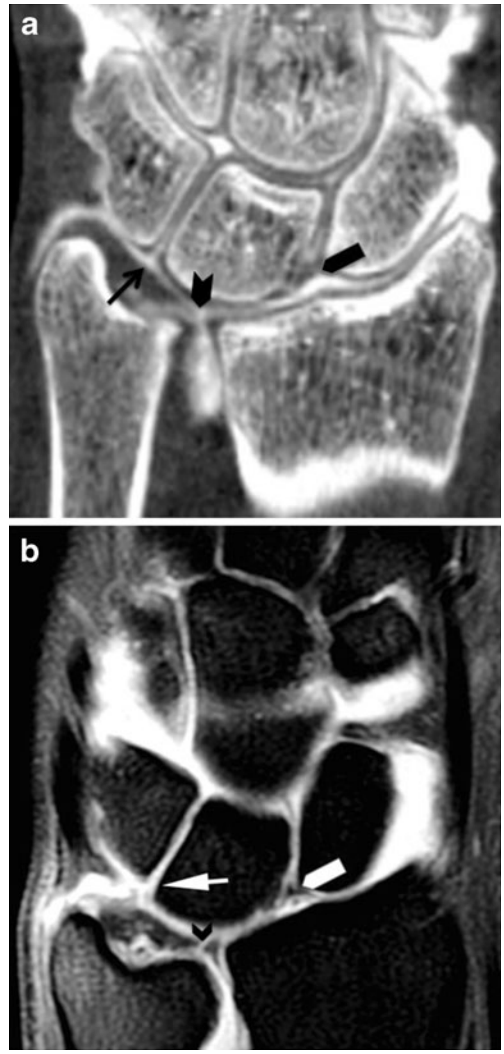

Fig. 5 TFC 1A (*arrowhead*) and LTL (*arrow*) tear. **a** Coronal CT-image (voxel size 0.4 × 0.4 × 0.4 mm^3) with **b** corresponding T1-w fat-saturated SE MR image (TR/TE 380/13 ms, FOV10cm, slice thickness 2.5 mm/2.7 space, matrix 256 × 192). SLL is intact (*block arrow*)

Discussion

CT arthrography is an alternative in patients when MRI is contraindicated or when MRI is not available.

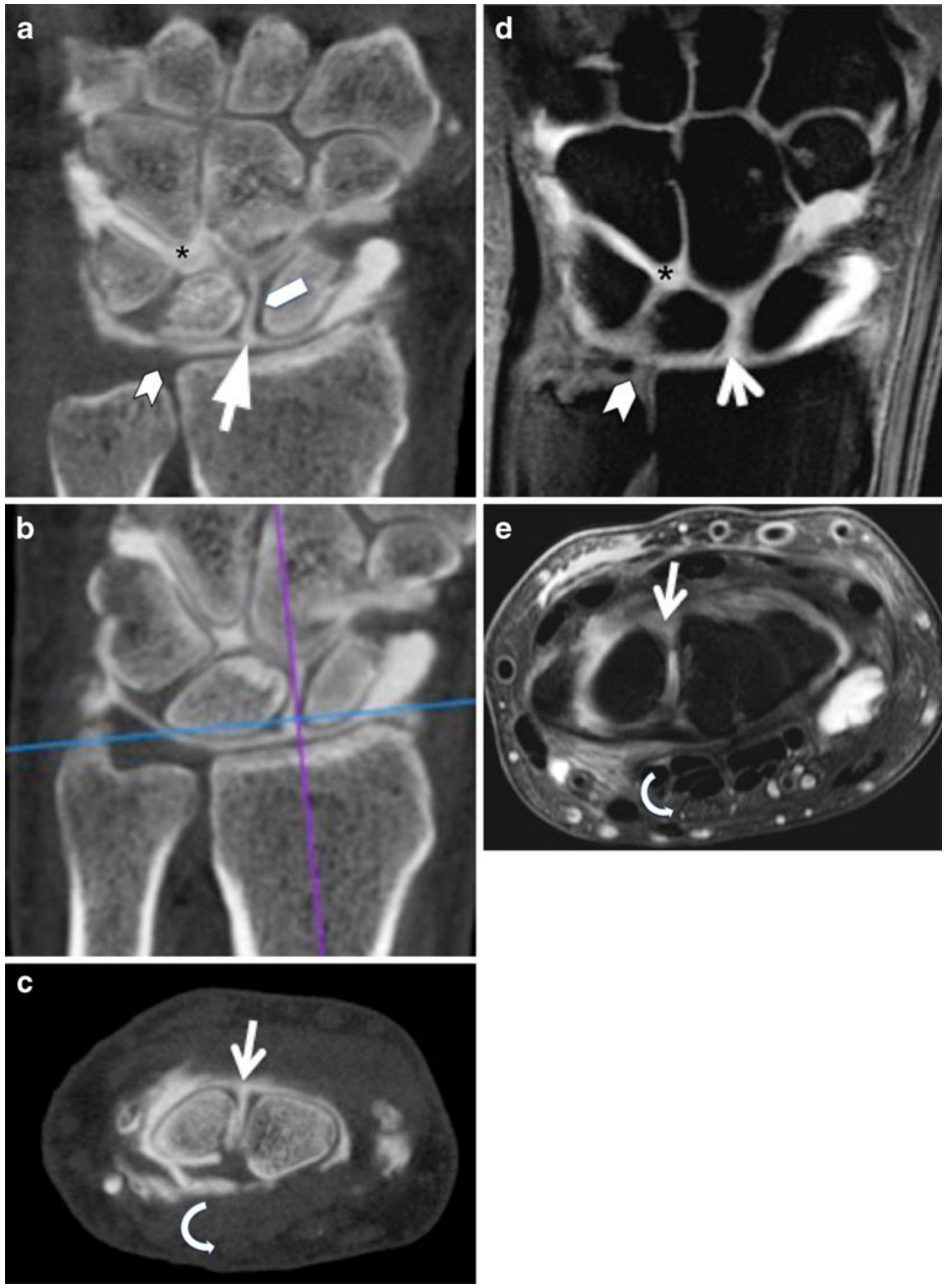

Fig. 6 SL-tear (*arrow*) in a 63-year-old male. **a** Coronal CT-image, **b** *blue line* shows the plane to create the axial plane in **c**. Corresponding coronal fat-saturated T1 SE (TR/TE 620/13 ms, FOV 10 cm, slice thickness 2.5 mm/2.7 space, FOV 10 cm, matrix 256×192 **d**) and **e** axial T2 FSE fat-saturated MR images (TR/TE eff. 2800/44 ms, slice thickness 3 mm/3.3 mm space, ETL 8, FOV 10 cm, matrix 320 × 192). Contrast leakage is seen to midcarpal joint (*asterisk*, **a**). No perforation in TFC (*arrowhead*; **a**, **d**) is seen. Note also the excellent visualization of cartilage (*block arrow*; **a**), whereas the soft-tissue contrast (**c**) is suboptimal compared to MRI (**e**). *Curved arrow* in **c**, **e** indicates the median nerve

Moreover, multi-detector CT (MDCT) arthrography has been reported to be more accurate than MRI or MR arthrography, especially in detecting partial tears of SL and LT ligaments [6]. In addition, experimental flat-panel C-arm CT arthrography has recently been reported [17]. In the current study, we used a novel, dedicated ambulatory cone-beam CT. Each study was technically successful, with overall accuracy of 82–86 %. This method offers exciting possibilities for orthopedic imaging in general. High spatial resolution, low radiation dose, and easy installation provide a potential one-stop shop for various orthopedic problems, such as subtle fracture detection and post-traumatic evaluation of fracture consolidation, especially when osteosynthetic material has been used [12]. Moreover, this technique allows imaging in a comfortable sitting position or even in patients lying on a hospital bed.

The spatial resolution used (0.4 mm^3) is superior to standard MR imaging where slice thickness is usually 2–3 mm and in-plane resolution 0.5–0.7 mm although

Table 2 Sensitivity (SENS), specificity (SPES), accuracy (ACC), positive predictive value (PPV), and negative predictive value (NPV) for scapholunate (SL), lunotriquetral (LT) ligament, and triangular fibrocartilaginous complex (TFCC) tears for readers 1 and 2. R1.1 and R2.1 denote first and second reader's first reading, and R1.2 and R2.2 the second readings, respectively

	R1.1	R1.2	R2.1	R2.2
SL				
SENS (%)	36	64	64	67
SPES (%)	95	98	88	85
ACC (%)	81	90	82	80
PPV (%)	67	88	58	57
NPV (%)	84	91	90	89
LT				
SENS (%)	100	75	86	71
SPES (%)	86	85	81	74
ACC (%)	88	84	82	73
PPV (%)	54	50	43	31
NPV (%)	100	95	97	94
TFCC				
SENS (%)	74	71	83	80
SPES (%)	87	91	90	87
ACC (%)	82	84	88	88
PPV (%)	78	80	83	80
NPV (%)	84	85	90	93

Table 3 Sensitivity (SENS), specificity (SPES), accuracy (ACC), positive predictive value (PPV), and negative predictive value (NPV) for cartilage abnormalities for scaphoid and lunate with corresponding radial surface for readers 1 and 2. *R1.1* and *R2.1* denote first and second reader's first reading, and R1.2 and R2.2 the second readings, respectively

	R1.1	R1.2	R2.1	R2.2
RADIUS (scaphoid fossa)				
SENS (%)	50	50	75	100
SPES (%)	94	91	94	98
ACC (%)	90	88	92	98
PPV (%)	40	40	50	80
NPV (%)	96	96	98	100
SCAPHOID				
SENS (%)	40	43	100	100
SPES (%)	89	91	96	100
ACC (%)	84	88	96	100
PPV (%)	29	43	71	100
NPV (%)	93	95	100	100
RADIUS (lunate fossa)				
SENS (%)	100	50	67	33
SPES (%)	89	91	90	96
ACC (%)	90	90	88	92
PPV (%)	29	20	29	33
NPV (%)	100	98	98	96
LUNATE				
SENS (%)	60	40	100	80
SPES (%)	95	93	85	96
ACC (%)	92	88	86	94
PPV (%)	60	40	42	67
NPV (%)	95	93	100	98

sub-millimeter isotropic voxels can also be obtained with 3.0-T scanners with gradient echo sequences, such as VIBE (volume interpolated breath-hold examination [18]). However, compared to MRI, the imaging time using CBCT is very short (18-s scan time) and patient positioning is easy, making it less prone to motion artifacts. Moreover, wrist CBCT arthrography could be an alternative in postoperative patients with radial volar plate fixation due to relative absence of metallic artifacts compared to MRI. The spatial resolution of the dedicated extremity CBCT is similar to MDCT scanners. However, due to limitations in low-contrast sensitivity of CBCT due to, e.g., scatter, soft-tissue contrast is lower compared to MDCT data. General challenges in CBCT contrast detectability, including scatter, beam hardening, truncation, and limited number of projections, can be partially corrected with calculation methods as reported for C-arm applications [19]. In the case of wrist imaging with FOV of 13 × 16 cm, the truncation effect is not a concern with the dedicated extremity CBCT.

According to dentomaxillofacial studies, the radiation doses of CBTC examinations are significantly lower compared to conventional MDCT scans [20–23]. The CBCT technique has also been previously used to detect finger fractures with equal accuracy as MDCT but with significantly less radiation [10]. Also, three cases of CBCT imaging of the wrist, including one with intra-articular contrast, has been reported [11]. The scanners used, however, represent a different design and technology than that used in the current study. Due to the target size and geometry of the X-ray beam in the scanner, conventional computed tomography dose index (CTDI) measures are not applicable to estimate the radiation exposure to the patient. Dose area product (DAP) also has limitations because the radiation beam area is wider than the wrist area. For typical exposure values used in the study (88-kV tube voltage, 8-mA tube current), DAP of 716 mGy*cm^2 was measured. For the wrist imaging, a conversion coefficient of 0.01 mSv/Gycm^2 [22] was used, providing an effective dose estimate of 7 μSv.

The inter- and intraobserver agreement was in most cases substantial. The fair interobserver agreement in SL ligament can be explained by the heterogeneity of our material with a substantial number with previous surgery and still-existing metal implants. In these cases, the distorted anatomy and postoperative changes interfered with the analysis even in retrospect. However, the study group was comprised of unselected material and is representative of a typical busy orthopedic practice. Also, the differences between readers most likely reflect the personal differences. In order to increase the specificity, reader 1 has, in general, lower sensitivity, and if the number of pathologic conditions is small, e.g., five in cartilage in lunate fossa (Table 3), one discordant reading may lead to substantial change in sensitivity. In addition, with an increasing prevalence, the values of the sensitivity and specificity of both observers have to increase in order to maintain a certain kappa value [24]. Therefore, a low kappa value, combined with a high prevalence of one of the categories, cannot be interpreted easily, and in such a case, the number of observations should be extended to make the prevalence of the categories more equally distributed [24].

The visualization of cartilage surface was excellent (Fig. 3), and provides a potentially good method of detecting cartilage injuries in the radiocarpal as well as other small joints, where cartilage thickness is in the order of 1 mm or less. While MR arthrography is good for detecting cartilage defects [25], arthroscopy is needed for a reference standard. It should be noted, however, that in case of orthopedic hardware, the visualization of cartilage with CBCT was better than with MR arthrography (Fig. 7)

In a previous study, CT arthrography was shown to have a very high (>90 %) sensitivity and specificity for SL, LT, and TFCC tears [6]. In our study, the corresponding numbers were slightly smaller, probably reflecting differences in the study population. They were also able to study partial tears, whereas in our study the amount of partial tears as well as the cartilage abnormalities was too small for a more detailed analysis.

The dedicated extremity CBCT scanner's low radiation dose, easy installation, and easy use open new possibilities for imaging of the radiocarpal joint. The use of CBCT arthrography and subsequent MR arthrography combines the inherent strengths of both methods; excellent visualization of bony structures and soft tissue contrast, respectively. Concomitant reading of both studies would potentially lead to increased diagnostic confidence and performance.

CT arthrography is recommended together with MR arthrography in order to increase the diagnostic accuracy of foveal tears and to assess the associated bone fragments [26].

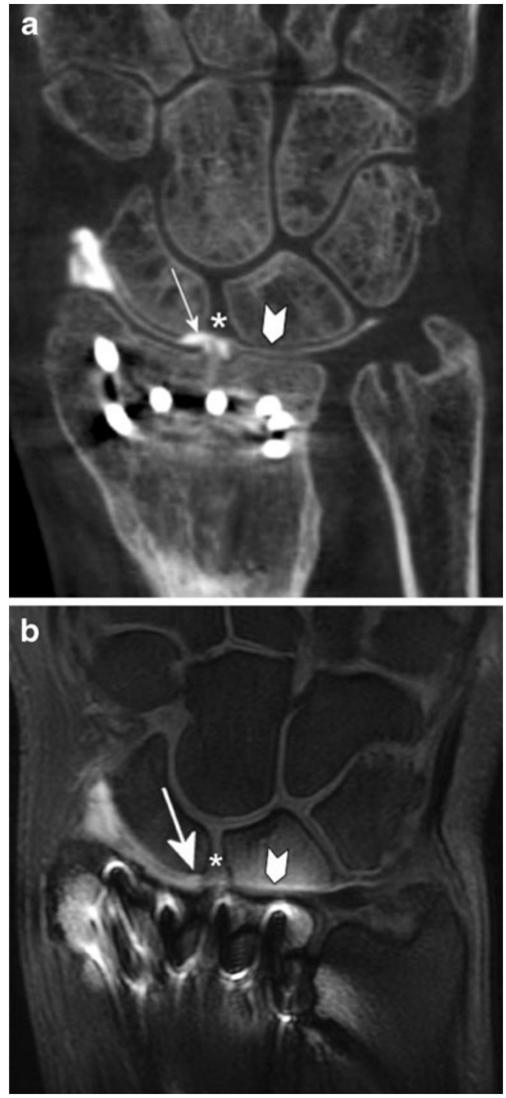

Fig. 7 In a patient with volar radial plate, ligament structures (SL-ligament; *asterisk*), wrist cartilage surface (especially in lunate, *arrowhead*) and a scaphoid cartilage defect (*arrow*) are better delineated on the coronal CT-image due to fewer metal artifacts (**a**) compared to corresponding T1-w fat-saturated SE MR image (**b**)

In conclusion, the dedicated CBCT extremity scanner is a new method for evaluating wrist ligaments. Moderate agreement was seen on articular cartilage for radius, scaphoid and lunate, and substantial agreement for LT ligament and TFCC. Interobserver agreement for SL ligament was fair. Intraobserver agreement for TFCC was almost perfect. The method has an accuracy of 82–86 % and specificity of 81–91 %. Sensitivity for LT and TFCC tears was 77–83 %, but for SLL tears it was 58 %. For cartilage abnormalities, the accuracy and negative predictive value were high, 90–98 %.

Acknowledgments Sharon J. Kuong, MD, is acknowledged for her linguistic help.

Conflict of interest The authors acknowledge that within the past 3 years they have received benefits which might result in a conflict of interest or the appearance of a conflict. Nature of benefit: Research Consultans (authors 1,3–5,7), employment (author 6).

References

1. Zlatkin MB, Chao PC, Osterman AL, Schnall MD, Dalinka MK, Kressel HY. Chronic wrist pain: evaluation with high-resolution imaging. Radiology. 1989;173:723–9.
2. Smith DK. MR imaging of normal and injured wrist ligaments. Magn Reson Imaging Clin N Am. 1995;3:229–48.
3. Golimbu CN, Firooznia H, Melone CP, Rafii M, Weinreb J, Leber C. Tears of the triangular fibrocartilage of the wrist: MR imaging. Radiology. 1989;173:731–3.
4. Hobby JL, Tom BD, Bearcroft PW, Dixon AK. Magnetic resonance imaging of the wrist: diagnostic performance statistics. Clin Radiol. 2001;56:50–7.
5. Haims AH, Moore AE, Schweitzer ME, Morrison WB, Deely D, Culp RW, et al. MRI in the diagnosis of cartilage injury in the wrist. Am J Roentgenol. 2004;182:1267–70.
6. Moser T, Dosch JC, Moussaoui A, Dietemann JL. Wrist ligament tears: evaluation of MRI and combined MDCT and MR arthrography. Am J Roentgenol. 2007;188:1278–86.
7. Cerezal L, de Dios Berná-Mestre J, Canga A, et al. MR and CT arthrography of the wrist. Semin Musculoskelet Radiol. 2012;16:27–41.
8. Mozzo P, Procacci C, Tacconi A, et al. A new volumetric CT machine for dental imaging based on the cone-beam technique: preliminary results. Eur Radiol. 1998;8:1558–64.
9. Arai Y, Tammisalo E, Iwai K, Hashimoto K, Shinoda K. Development of compact computed tomographic apparatus for dental use. Dentomaxillofac Radiol. 1999;28:245–8.
10. De Vos W, Casselman J, Swennen GRJ. Cone-beam computerized tomography (CBCT) imaging of the oral and maxillofacial region: a systematic review of the literature. Int J Oral Maxillofac Surg. 2009;38:609–25.
11. Faccioli N, Foti G, Barillari M, Atzei A, Mucelli RP. Finger fractures imaging: accuracy of cone-beam computed tomography and multislice computed tomography. Skeletal Radiol. 2010;39:1087–95.
12. De Cock J, Mermuys K, Goubau J, van Petegem S, Houthoofdt B, Casselman JW. Cone-beam computed tomography: a new low-dose, high-resolution imaging technique of the wrist, presentation of three cases with technique. Skeletal Radiol. 2012;41:93–6.
13. Zbijewski W, De Jean P, Prakash P, et al. A dedicated cone-beam CT system for musculoskeletal extremities imaging: design, optimization, and initial performance characterization. Med Phys. 2011;38:4700–13.
14. Mattila KT, J. Kankare J, Kortesniemi M, et al. Cone beam CT for extremity imaging. EPOS Abstract, ECR 2011, Vienna March 3–7, 2011. doi:10.1594/ecr2011/C-0297.
15. Biswas D, Bible JE, Bohan M, Simpson AK, Whang PG, Grauer JN. Radiation exposure from musculoskeletal computerized tomographic scans. J Bone Joint Surg Am. 2009;91:1882–9.
16. Landis JR, Koch GG. The measurement of observer agreement for categorial data. Biometrics. 1997;33:159–74.
17. Guggenberger R, Fischer MA, Hodler J, Pfammatter T, Andreisek G. Flat-panel CT-arthrography. Feasibility study and comparison to multidetector CT arthrography. Invest Radiol. 2012;47:312–8.
18. Zheng Z-Z, Shan H, Li X. Fat-suppressed 3D T1-weighted gradient-echo imaging of the cartilage with a volumetric interpolated breath-hold examination. Am J Roentgenol. 2010;194:W414–9.
19. Heigl B, Kowarschik M. High-Speed> Reconstruction for C-Arm Computed Tomography. In Proceedings of the 9th International Meeting on Fully Three-Dimensional Image Reconstruction in Radiology and Nuclear Medicine, pp. 25–28, Lindau, Germany, July 2007.
20. Tsiklakis K, Donta C, Gavala S, Karayianni K, Kamenopoulou V, Hourdakis CJ. Dose reduction in maxillofacial imaging using low-dose cone-beam CT. Eur J Radiol. 2005;56:413–7.
21. Roberts JA, Drage NA, Davies J, Thomas DW. Effective dose from cone-beam CT examinations in dentistry. Br J Radiol. 2009;82:35–40.
22. Koong B. Cone-beam imaging: is this the ultimate imaging modality? Clin Oral Implants Res. 2010;21:1201–8.
23. Hart D, Wall BF. Radiation Exposure of the UK population from Medical and Dental X-ray Examinations; Report NRPB-W4; National Radiological Protection Board, UK; 2002.
24. Donker DK, Hasman A, van Geijn HP. Interpretation of low kappa values. Int J Biomed Comp. 1993;33:55–64.
25. Scheck RJ, Romagnolo A, Hierner R, Pfluger T, Wilhelm K, Hahn K. The carpal ligaments in MR arthrography of the wrist: correlation with standard MRI and wrist arthroscopy. J Magn Reson Imaging. 1999;9:468–74.
26. Omlor G, Jung M, Grieser T, Ludwig K. Depiction of the triangular fibro-cartilage in patients with ulnar-sided wrist pain: comparison of direct multi-slice CT arthrography and direct MR arthrography. Eur Radiol. 2009;19:147–51.